# Synthesis of Cp′Ru(CO)(L)($\eta^2$-olefin)$^+$ Complexes and Kinetic Studies of Olefin Substitution

Kevin M. McWilliams, Arkady Ellern,† and Robert J. Angelici*

*Department of Chemistry, Iowa State University, Ames, Iowa 50011-3111*

*Received December 1, 2006*

The ruthenium(II)−olefin complexes [Cp′Ru(CO)(L)($\eta^2$-olefin)]$^+$ (Cp′ = Cp, Cp*; L = CO, $PPh_3$; olefin = methyl oleate, *cis*-3-hexene, *trans*-3-hexene, 1,4-pentadiene) have been synthesized and characterized by IR and $^1$H and $^{13}$C NMR spectroscopy. An X-ray structure of [CpRu(CO)($PPh_3$)($\eta^2$-*cis*-3-hexene)]$^+$ shows that the olefinic bond is nearly parallel to the plane of the Cp ligand. The olefins in [CpRu(CO)$_2$($\eta^2$-*trans*-3-hexene)]$^+$ and [Cp′Ru(CO)$_2$($\eta^2$-*trans*-3-hexene)]$^+$ rotate rapidly about the Ru−olefin bond, even at −30 °C, as established by the presence of a single methyl signal for the olefin in the $^1$H NMR spectrum, whereas olefin rotation in [CpRu(CO)($PPh_3$)($\eta^2$-*trans*-3-hexene)]$^+$ is slow on the $^1$H NMR time scale at −25 °C. The [CpRu(CO)($PPh_3$)]$^+$ unit exhibits a unique diastereoselectivity by binding to only one face of *trans*-3-hexene, due to steric repulsion between the ethyl groups of the *trans*-3-hexene and the bulky Cp and $PPh_3$ ligands. Kinetic studies of the substitution of the olefin in [Cp'Ru(CO)$_2$($\eta^2$-olefin)]$^+$ by $PPh_3$ show that the lability of the large methyl oleate is similar to that of the smaller *cis*-3-hexene. Replacement of Cp by Cp* and of *cis*-3-hexene by *trans*-3-hexene increases substantially the rate of olefin substitution, due to an increase in steric repulsion.

## Introduction

Transition-metal−olefin complexes of the type [CpFe(CO)$_2$($\eta^2$-olefin)]$^+$ (Cp = $C_5H_5$) can be prepared by a number of methods such as alkene exchange,[1] displacement of water from [CpFe(CO)$_2$(OH$_2$)]$^+$,[2] oxidation of [CpFe(CO)$_2$]$_2$,[3] and halide abstraction from CpFe(CO)$_2$I.[4] These complexes are useful as models for catalytic intermediates as well as reagents in organic synthesis.[5] The ruthenium analogues are not nearly as well studied in either the number of compounds or investigations of their reactivity.[6] Known compounds of the type [CpRu(CO)$_2$($\eta^2$-olefin)]$^+$ (olefin = ethylene, propene, cyclohexene, 1-pentene, 1-hexadecene)[7] are relatively few, which may be attributed to the limited synthetic techniques that have been employed, almost all of which center on using a Lewis acid in the presence of excess olefin.[8]

Recently our group reported equilibrium constants for $\eta^2$ coordination of several unsaturated fatty acid methyl esters (methyl oleate (18:1), methyl linoleate (18:2), and methyl linoleneate (18:3)) and smaller olefins (*cis*-3-hexene and 1,4-pentadiene) in [CpPd($PR_3$)($\eta^2$-olefin)]$^+$ complexes.[9] None of the complexes of the unsaturated fatty esters were sufficiently stable to be isolated. On the basis of previous reports of [CpRu(CO)$_2$($\eta^2$-olefin)]$^+$ complexes, it appeared that it may be possible to isolate analogous complexes of the unsaturated fatty esters and compare the kinetic lability of $\eta^2$-methyl oleate (18:1, *cis*-$CH_3(CH_2)_7CH{=}CH(CH_2)_7CO_2Me$) with smaller olefins in a series of [CpRu(CO)$_2$($\eta^2$-olefin)]$^+$ complexes. The ability of ruthenium to successfully bind large olefins has been detailed in a recent study, in which $Ph_3C[PF_6]$ was used to abstract a hydride from CpRu(CO)$_2$($\eta^1$-$C_{16}H_{33}$) to yield [CpRu(CO)$_2$($\eta^2$-$CH_2{=}CH(CH_2)_{13}CH_3$)]$^+$.[10]

Herein we report the synthesis and characterization of a series of ruthenium−olefin complexes of the type [Cp′Ru(CO)(L)($\eta^2$-olefin)]$^+$, where Cp′ = Cp, Cp* and L = CO, $PPh_3$, with a focus on defining the orientation and rotational fluxionality of the olefin and diastereoselectivity of the [CpRu(CO)($PPh_3$)]$^+$ unit for binding one face of the olefin. Kinetic studies of the displacement of the olefin in the [Cp′Ru(CO)$_2$($\eta^2$-olefin)]$^+$ complexes by $PPh_3$ were performed in an effort to determine the structural effects of the olefin and Cp′ ligand on the lability of the olefin.

## Results and Discussion

**Synthesis and Structural Characterization of the [Cp′Ru(CO)(L)($\eta^2$-olefin)]$^+$Y$^-$ Complexes.** These complexes were all prepared by the abstraction of Cl$^-$ from Cp′Ru(CO)(L)Cl, where L = CO, $PPh_3$ and Cp′ = Cp ($\eta^5$-$C_5H_5$), Cp* ($\eta^5$-$C_5Me_5$), in the presence of the desired olefin (Scheme 1).

* To whom correspondence should be addressed. E-mail: angelici@iastate.edu. Tel: 515-294-2603. Fax: 515-294-0105.

† Molecular Structure Laboratory, Iowa State University, Ames, IA 50011-3111.

(1) (a) Ishii, Y.; Kagayana, T.; Inada, A.; Ogawa, M. *Bull. Soc. Chem. Jpn.* **1983**, *56*, 2861. (b) Marsi, M.; Rosenblum, M. *J. Am. Chem. Soc.* **1984**, *106*, 7264. (c) Rosenblum, M.; Turnbull, M. M.; Foxman, B. M. *Organometallics* **1986**, *5*, 1062.

(2) Tahiri, A.; Guerchais, V.; Toupet, L.; Lapinte, C. *J. Organomet. Chem.* **1990**, *381*, C47.

(3) Krivykh, V. V.; Gusev, O. V.; Peterleitner, M. G.; Denisovitch, L. I.; Rybinskaya, M. I. *Chem. Abstr.* **1987**, *106*, 120.

(4) Reger, D. L.; Belmore, K. A.; Mintz, E.; Charles, N. G.; Griffith, E. A. H.; Amma, E. L. *Organometallics* **1983**, *2*, 101.

(5) Davies, S. G. *Organotransition Metal Chemistry: Applications to Organic Synthesis*; Pergamon Press: Oxford, England, 1982.

(6) Bennett, M. A.; Bruce, M. I.; Matheson, T. W. In *Comprehensive Organometallic Chemistry*; Wilkinson, G., Stone, F. G. A., Abel, E. W., Eds.; Pergamon Press: Oxford, England, 1982; Vol. 4.

(7) (a) Jungbauer, A.; Behrens, H.; *Z. Naturforsch., B* **1978**, *33*, 1083. (b) Fischer, E. O.; Vogler, A. *Z. Naturforsch., B* **1962**, *17*, 421.

(8) Bennett, M. A.; Khan, K.; Wenger, E. In *Comprehensive Organometallic Chemistry II*; Abel, E. W., Stone, F. G. A., Wilkinson, G., Shriver, D. F., Bruce, M. I., Eds.; Pergamon Press: Oxford, England, 1995; Vol. 7.

(9) Ghebreyessus, K. Y.; Ellern, A.; Angelici, R. J. *Organometallics* **2005**, *24*, 1725.

(10) Clayton, H. S.; Moss, J. R.; Dry, M. E. *J. Organomet. Chem.* **2003**, *688*, 181.

10.1021/om061096u CCC: $37.00 
Publication on Web 03/03/2007

**Scheme 1**

$$Cp'Ru(CO)(L)Cl + \text{olefin} \xrightarrow[-AgCl]{AgY,\ CH_2Cl_2} [Cp'Ru(CO)(L)(\eta^2\text{-olefin})]^+Y^- \quad \mathbf{1-12}$$

For Cp′ = Cp, L = CO, Y = $BF_4$: olefin = 18:1 (**1**), c3hx (**2**), t3hx (**3**), 1,4ptd (**4**)

For Cp′ = Cp*, L = CO, Y = $PF_6$: olefin = 18:1 (**5**), c3hx (**6**), t3hx (**7**), 1,4ptd (**8**)

For Cp′ = Cp, L = $PPh_3$, Y = $PF_6$: olefin =18:1 (**9**), c3hx (**10**), t3hx (**11**), 1,4ptd (**12**)

18:1 = *cis*-$CH_3(CH_2)_7CH{=}CH(CH_2)_7CO_2Me$; c3hx = *cis*-3-hexene; t3hx = *trans*-3-hexene; 1,4ptd = 1,4-pentadiene

The general structures of the synthesized compounds are shown in Figure 1. With the exception of **5** and **9**, all products were isolated as either light tan or light yellow solids. Complexes **5** and **9** were isolated as a dark brown oil and a dark yellow oil, respectively. All of the solid compounds, with the exception of **8**, are stable indefinitely as solids and stable for several days if left in solution open to air.

In the $\nu$(CO) region of their IR spectra, complexes **1**−**3** have two peaks that appear at ∼2077 and ∼2034 $cm^{-1}$; these absorptions occur at slightly higher values of 2083 and 2040 $cm^{-1}$ in the 1,4ptd complex **4**. Complexes **5**−**8** exhibit $\nu$(CO) values (∼2062 and ∼2018 $cm^{-1}$) that are about 15 $cm^{-1}$ lower than those in the analogous Cp complexes **1**−**4**, due to the stronger electron-donating ability of the Cp* ligand.[11] The $PPh_3$-substituted complexes **9**−**11** give one $\nu$(CO) peak at ∼2003 $cm^{-1}$, whereas the 1,4ptd complex **12** is again slightly higher at 2006 $cm^{-1}$. In the compounds **1**, **5**, and **9** of 18:1, the $\nu$(C═O) value of the ester group is the same as that (1732 $cm^{-1}$) in free methyl oleate, which indicates that the Ru does not bind to the ester group. The preference for ruthenium binding to an olefin in the presence of an ester group has been shown previously in the [CpRu{$Ph_2PCH(CH_3)CH(CH_3)PPh_2$}($\eta^2$-$H_2C{=}CH(CO_2Me)$]$^+$ complex.[12]

An X-ray structure determination of **10** shows that the crystal diffraction data were consistent with the space groups *P*1 and $P\bar{1}$ (Table 1). The *E* statistics strongly suggested the centrosymmetric space group *P*1, which yielded chemically reasonable and computationally stable refinement results. Two molecules of **10,** two counterions, and one molecule of $CH_2Cl_2$ solvent were found in an asymmetric unit of the triclinic cell, showing the existence of both enantiomers in the crystal lattice. The ORTEP drawing for one of them is shown in Figure 2. Both enantiomers assume a three-legged piano-stool geometry. The double bond of the *cis*-3-hexene ligand is approximately parallel to the Cp ring, having a tilt angle ($\theta$) of 94.6°, which is defined by the angle between the Ru(1)−C(26)═C(27) plane and the plane defined by the Cp centroid, Ru(1), and the C(26)═C(27) centroid (Figure 3A). Both ethyl groups in **10** point up toward but away from the cyclopentadienyl ring. The Ru(1)−C(26) and Ru(1)−C(27) bond lengths (2.285(5) and 2.304(5) Å, respectively) are the same within experimental error. The C26−C27 bond distance (1.367(8) Å) is slightly longer than that (1.337 Å) of free ethylene.[13] The olefinic C═C distance in **10** is shorter than that (1.416(13) Å) in [Cp*Ru(CO)($PMe^iPr_2$)($\eta^2$-ethene)]$^+$ (**13**), presumably because the higher electron density provided by the Cp* and phosphine ligands increases $\pi$ back-bonding to the olefin in **13**.[14] The tilt angle ($\theta$) is slightly larger (99.2°) for **13** in comparison to the angle (94.6°) in **10**. In both compounds, the olefins tilt away from the $PR_3$ ligand, with the larger tilt in **13** being attributed to the lack of R groups on the olefin, permitting the ethylene to rotate closer to the Cp ring. The P(1)−Ru(1)−C(26) angle (85.50(15)°) is greater than the C(30)−Ru−C(27) angle (78.34(2)°) in **10**. This difference may be attributed to the larger size of the $PPh_3$ ligand forcing the olefin toward the smaller carbonyl ligand, as was also suggested for **13**. The torsion angles C(25)−C(26)−C(27)−H(27a) (140°) and C(28)−C(27)−C(26)−H(26a) (−143°) in **10** are smaller than that predicted for the free olefin (180°), which indicates that the substituents on the olefinic carbons are bent out of the $\pi$ nodal plane upon binding to the metal fragment.

Previous studies of [Cp′M$(CO)_2$(olefin)]$^+$ (M = Fe, Ru) by Faller and Johnson showed the preferred orientation of the olefins in these systems to be approximately parallel to the Cp ring.[15] This assignment was based on low-temperature NMR studies of the complexes where Cp′ was an indenyl group. For the propene complex, estimated shifts for the olefinic protons $H_a$, $H_b$, and $H_c$ were calculated on the basis of a geometric model and shielding effects caused by ring currents. It was found that both propene and *trans*-2-butene in their iron complexes likely assume an approximate tilt angle of 100° to reduce the steric interaction of the methyl groups with the indenyl ligand. For *cis*-2-butene, the NMR data suggested a tilt angle of 90° in which both methyl groups are directed toward the less bulky carbonyl ligands. At 94.6° the tilt angle of *cis*-3-hexene in **10** is similar to those in the aforementioned complexes. Therefore, in **10**, the *cis*-3-hexene is approximately parallel to the Cp ring, as is the case for the *cis*-2-butene in Faller's studies, but the ethyl groups in **10** point toward the Cp ring rather than away from it in the [Cp′Fe$(CO)_2$($\eta^2$-olefin)]$^+$ complexes, owing to the bulkiness of the $PPh_3$ in **10**.

Results of studies of [CpRe(NO)($PPh_3$)($\eta^2$-olefin)]$^+$ (**14**) with monosubstituted ($CH_2$═CHR) and disubstituted olefins (CHR═CHR′) have led to the proposal that the double bond of the olefin prefers to align with the Re−P vector to maximize $\pi$ back-bonding to the olefin.[16] The tilt angle ($\theta$) in an idealized structure would be 45° (Figure 3B). From X-ray diffraction studies of the complexes with styrene, *cis*-2-butene, and *trans*-2-butene, the tilt angles were found to be 65, 64.2, and 71.8°, respectively.[17] Deviations from the ideal angle of 45° were attributed to minimizing the steric interactions between the olefin R groups and both the $PPh_3$ and Cp ligands. The tilt angle of 94.6° in **10** as compared to 64.2° in [CpRe(NO)($PPh_3$)(*cis*-2-butene)]$^+$ suggests that steric interactions play a more important role than electronic factors in **10**, as $\pi$ back-bonding in both the Ru and Re systems would be maximized at an angle of 45°. The greater importance of steric repulsions in **10** may be attributed to the smaller size of the Ru atom, as indicated by the shorter Ru−P bond (2.336(2) Å) in comparison to the Re−P bond (2.426(1) Å), resulting in a more congested environment around Ru

(11) Friedrich, H. B.; Makhesha, P. A.; Moss, J. R.; Williamson, B. K. *J. Organomet. Chem.* **1990**, *384*, 325.
(12) Consiglio, G.; Pregosin, P.; Morandini, F. *J. Organomet. Chem.* **1986**, *308*, 345.
(13) Bartell, L. S.; Roth, E. A.; Hollowell, C. D.; Kuchitsu, K.; Young, J. E., Jr. *J. Chem. Phys.* **1965**, *42*, 2683.
(14) Jimenez-Tenorio, M.; Palacies, M. D.; Puerta, M. C.; Valerga, P. *Organometallics* **2004**, *23*, 504.
(15) Faller, J. W.; Johnson, B. V. *J. Organomet. Chem.* **1975**, *88*, 101.
(16) Peng, T.; Gladysz, J. A. *J. Am. Chem. Soc.* **1992**, *114*, 4174.
(17) (a) Bocher, G. S.; Peng, T.; Arif, A. M.; Gladysz, J. A. *Organometallics* **1990**, *9*, 1191. (b) Pu, J.; Peng, T.; Mayne, C. L.; Arif, A. M.; Gladysz, J. A. *Organometallics* **1993**, *12*, 2686.

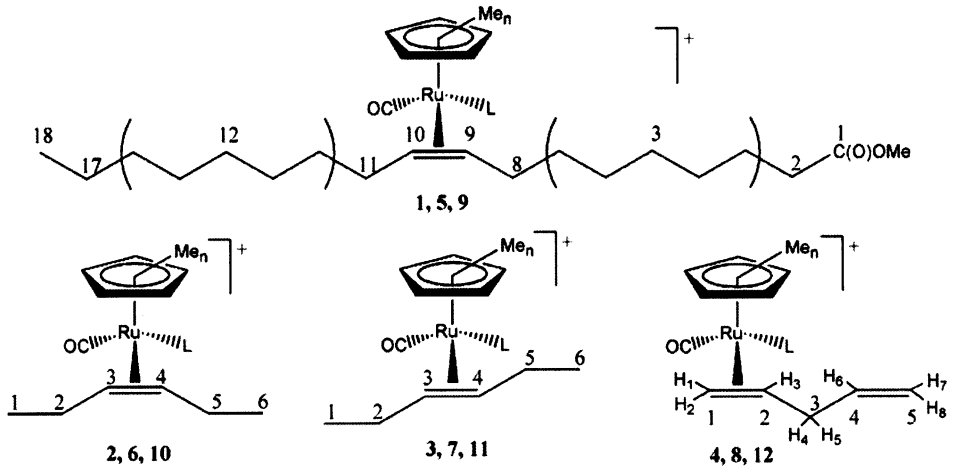


**Figure 1.** Structures of compounds **1**−**12**. Carbon and hydrogen labels correspond to NMR assignments given in the Experimental Section.

**Table 1. Crystal Data and Structure Refinement Details for [(η⁵-C₅H₅)Ru(CO)(PPh₃)(η²-c3hx)][PF₆] (10)**

| | |
|---|---|
| empirical formula | $C_{30}H_{32}OP_2F_6Ru\cdot0.5CH_2Cl_2$ |
| fw | 728.03 |
| cryst syst | triclinic |
| space group | $P\bar{1}$ |
| unit cell dimens | |
| *a* | 9.522(2) Å |
| *b* | 17.427(4) Å |
| *c* | 19.654(4) Å |
| α | 83.043(4)° |
| *β* | 83.922(4)° |
| *γ* | 78.551(3)° |
| *V* | 3161.8(11) Å³ |
| *Z* | 4 |
| density (calcd) | 1.529 Mg/m³ |
| abs coeff | 0.740 mm⁻¹ |
| *F*(000) | 1476 |
| no. of rflns collected | 24 803 |
| max, min transmissn | 1, 0.79 |
| no. of data/restraints/params | 12 791/0/748 |
| goodness of fit on $F^2$ | 1.027 |
| final $R^a$ indices ($I > 2\sigma(I)$) | R1 = 0.0574, wR2 = 0.1529 |
| $R^a$ indices (all data) | R1 = 0.0925, wR2 = 0.1741 |
| largest diff peak, hole | 2.018, −1.253 e Å⁻³ |

[a] $R1 = \sum||F_o| - |F_c||/\sum|F_o|$ and $wR2 = \{\sum[w(F_o^2 - F_c^2)^2]/\sum[w(F_o^2)^2]\}^{1/2}$.

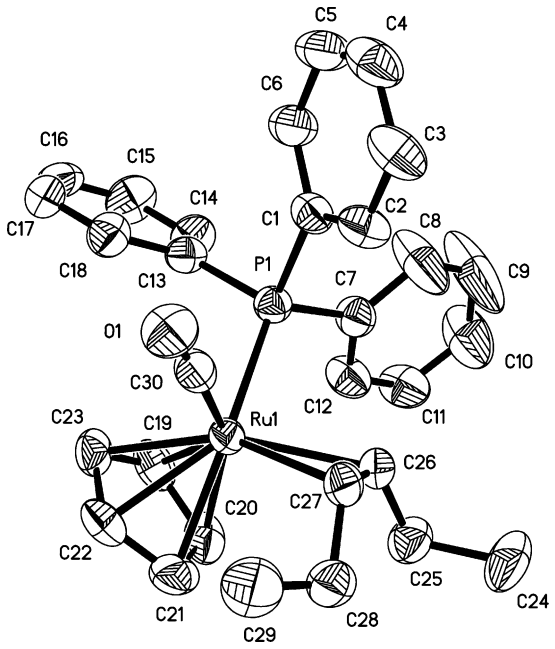


**Figure 2.** ORTEP drawing of one of the independent [CpRu(CO)(PPh₃)(c3hx)]⁺ enantiomers in **10**, showing the atom-numbering scheme (50% probability thermal ellipsoids). Hydrogen atoms are omitted for clarity. Selected bond lengths (Å): Ru(1)−C(26), 2.285(5); Ru(1)−C(27), 2.304(5); Ru(1)−P(1), 2.336(2); Ru(1)−C(30), 1.871(6); C(26)−C(27), 1.367(8). Selected bond angles (deg): Ru(1)−C(26)−C(27), 73.4(3); Ru(1)−C(27)−C(26), 71.9(3); C(26)−Ru(1)−P(1), 85.50(15); C(27)−Ru(1)−C(30), 78.34(2); Ru(1)−C(26)−C(25), 117.4(4); Ru(1)−C(27)−C(28), 116.0(4); P(1)−Ru(1)−C(30), 88.68(17); C(26)−C(27)−C(28), 125.9(5); C(25)−C(26)−C(27), 124.4(5).

leading to a greater tilt angle to relieve strain within the complex. A notable difference between **14** and **10** is the orientation of the R groups in the olefin. In the Re complex, the methyl groups on the butene point away from the Cp ring (Figure 3B), whereas the ethyl groups in **10** point toward the Cp (Figure 3A). As described by Gladysz,[17a] electronic factors in the rhenium complex primarily control the olefin orientation, while steric interactions play a secondary role. Therefore, the *cis*-2-butene methyl groups are directed away from both the Cp and $PPh_3$ ligands in order to minimize steric congestion and allow for an angle close to 45° to maximize back-bonding. On the other hand, steric interactions are most important in **10**, which lead to the ethyl groups pointing up toward and away from the Cp to minimize interactions with the $PPh_3$ ligand, which has been noted in previous work as being more sterically demanding than a Cp ring.[17b] The similarity of the tilt angles in [Cp*Ru(CO)(PMeⁱPr₂)(η²-ethene)]⁺ (**13**) (99.2°) and **10** (94.6°) suggests that steric factors are more important in **13** also.

**[Cp′Ru(CO)(L)(η²-c3hx)]Y Complexes (2, 6, and 10).** In the $^1$H NMR spectrum of **2**, there is a modest shift upfield from 5.35 to 5.21 ppm for the olefinic protons in c3hx upon binding to the $[CpRu(CO)_2]^+$ fragment. This is consistent with chemical shifts of other known olefin complexes of ruthenium: e.g., $[CpRu(CO)_2(C_2H_4)]^+$, $[CpRu(CO)_2(C_3H_6)]^+$, and $[CpRu(CO)_2(C_6H_{10})]^+$.[7] In the $^1$H NMR spectrum of **2**, only one methyl signal at 1.25 (t) ppm is observed for the bound olefin, but there are two methylene multiplets at 2.28 and 2.08 ppm; the free olefin exhibits a single multiplet at 2.05 ppm for the $CH_2$ protons. Cooling a sample of **2** in acetone-$d_6$ to −35 °C failed to broaden the olefinic proton peaks. $^1$H−$^1$H COSY experiments show that the two hydrogens on the same methylene carbon are different and are coupled to each other. This inequivalence is consistent with the structure **A** (Figure 4), in which the C═C olefin bond is parallel to the Cp ring, but it is not consistent with the static perpendicular orientation **B**, in which all four methylene protons would be inequivalent. The observation of two methylene $^1$H NMR signals is not only consistent with a

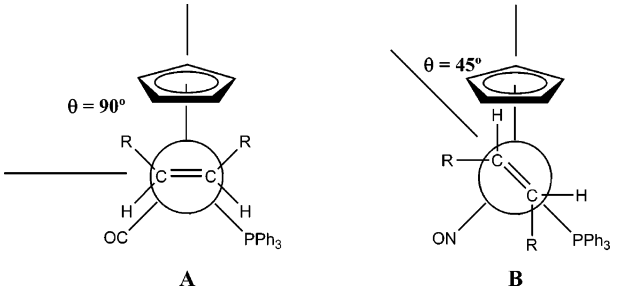


**Figure 3.** Structure of $[CpRu(CO)(PPh_3)(CHR{=}CHR)]^+$ (**A**), depicting a tilt angle of 90°, and structure of $[CpRe(NO)(PPh_3)(CH_2{=}CHR)]^+$ (**B**), showing the idealized 45° tilt angle.

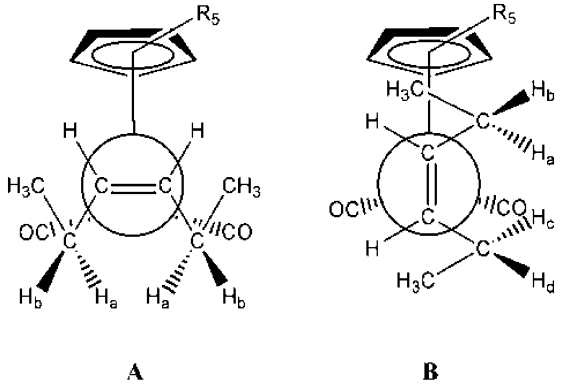


**Figure 4.** Parallel (**A**) and perpendicular (**B**) orientations of *cis*-3-hexene with respect to the Cp ring, showing the different methylene protons.

static parallel structure but would also be consistent with a structure in which the olefin is rapidly rotating. Rotation occurs in both **13** as well as in many of the $[CpRe(NO)(PPh_3)(\eta^2\text{-olefin})]^+$ compounds, some of which must be cooled to −100 °C in order to distinguish between diastereomers. On the basis of the nearly parallel structures of **10** and **13** in the solid state, it seems likely that the olefin in **2** is parallel to the Cp, but unlike the structure of **10**, the ethyl groups are probably directed away from the Cp ring (**A** in Figure 4) because of the absence of the bulky $PPh_3$ ligand that is present in **10**. However, it is not possible to state whether structure **A** for **2** is static or the olefin is rotating rapidly. This is also the situation for complexes **1**, **2**, **4**−**6**, **8**−**10**, and **12**. Only for the complexes of t3hx (**3**, **7**, **11**) is it possible to conclude that the olefin is rotating rapidly on the NMR time scale at room temperature.

At 3.86 ppm the olefinic protons of compound **6** are upfield as compared with those (5.21 ppm) in **2**, due to the greater electron donation by the Cp* ligand. As in **2**, **6** has only one methyl signal for the *cis*-3-hexene at 1.22 ppm, but there are again two methylene signals at 2.20 and 2.12 ppm that are coupled to one another. In compound **10**, the chiral ruthenium gives rise to two distinct olefin multiplets at 3.88 and 3.49 ppm for the *cis*-3-hexene ligand. There are again two methylene resonances at 2.12 and 1.83 ppm, with the former being almost resolved into two separate multiplets. The hydrogen atoms on carbon 2 (Figure 1) located closer to the CO ligand are expected to be different from those on carbon 5, which will be closer to the $PPh_3$ ligand. The methylene hydrogens on carbons 2 and 5 will also be different from one another, as observed in **2** and **6**. Therefore, one expects four separate resonances for the methylene hydrogen atoms in **10**. The methylene peak at 2.12 ppm shows only a cross-peak with the olefin proton at 3.88 ppm, whereas the methylene peak at 1.83 ppm shows only a cross-peak with the olefin proton at 3.49 ppm. Thus, each methylene peak may be assigned to protons on the same carbon due to the coupling with only one olefinic proton; the absence of a cross-peak between the methylene peaks is presumably due to the five-bond separation. Shifts of the methylene protons in **10** are determined more by the neighboring ligands (CO or $PPh_3$) than by the direction the methylene protons are pointing. The $^1$H NMR spectrum of **10** in solution is consistent with parallel binding of the olefin, as shown in the structure determined by X-ray diffraction.

**[Cp′Ru(CO)(L)($\eta^2$-18:1)]Y Complexes (1, 5, and 9).** As in **2**, the bound olefin signals in **1** are observed upfield of free methyl oleate (5.32 ppm) at 5.15 ppm. Larger shifts occur in the $^{13}$C NMR spectrum, where the olefinic carbons ($C_9$ and $C_{10}$) are shifted upfield from approximately 130 ppm in free methyl oleate to 81.04 and 80.88 ppm in the bound form. Two discrete $^{13}$C peaks for the CO ligands appear at 195.15 and 195.08 ppm, indicating the asymmetry of the methyl oleate ligand as well as the absence of rapid dissociation and reassociation of the olefin that would result in the CO groups becoming equivalent. Complex **1** is stable with respect to air and moisture in solution for several days; as a sticky solid, the compound did not degrade noticeably over several months. The sticky composition is likely due to the flexibility of the long hydrocarbon chain in the methyl oleate ligand. Low-temperature (−35 °C) $^1$H NMR studies of **1** in acetone-$d_6$ did not show significant broadening of the olefin peak. The long pendant groups of the methyl oleate pose a larger steric problem to rotation than do the ethyl groups in *cis*-3-hexene, but rotational fluxionality cannot be ruled out. To the best of our knowledge, this is the first isolated and characterized transition-metal complex of methyl oleate.

The influence of the Cp* ligand in **5** is clearly seen in the $^1$H NMR spectrum, where the olefin signal (3.88 ppm) of the methyl oleate is much further upfield than in **1** (5.15 ppm). Methylene splitting occurs as in the previously discussed compounds with resonances at 2.10 and 1.95 ppm, and two carbon signals for the inequivalent CO ligands in the $^{13}$C NMR spectrum occur at 198.51 and 198.47 ppm, which is similar to those in **1** (195.15, 195.08 ppm).

The $^1$H NMR spectrum of **9** shows two olefinic protons (3.80 and 3.48 ppm) further upfield than those in **1**. The upfield peak at 3.48 ppm may be assigned to the olefinic proton nearest the $PPh_3$ ligand, whose phenyl rings would be expected to shield this proton.[17b]

**[Cp′Ru(CO)(L)($\eta^2$-t3hx)]Y Complexes (3, 7, and 11).** In the $^1$H NMR spectrum of **3**, the methyl groups are observed as a single triplet at 1.17 ppm, but two methylene resonances are observed at 2.23 and 1.64 ppm. $^1$H−$^1$H COSY spectra show that these signals arise from two protons on the same methylene carbon. The appearance of two CO peaks in the $^{13}$C NMR spectrum at 197.02 and 192.58 ppm is in contrast to the case for compound **2,** which exhibits only a single CO peak at 194.85 ppm. If the t3hx were locked into a parallel orientation (**A** in Figure 4), the methylene groups would be inequivalent and therefore appear as two signals. The appearance of only one methyl signal, combined with the sharpness of the peaks, indicates a fast rotation of the olefin about the metal−olefin bond. Fast rotation, in this case, would not make the two CO peaks equivalent in the $^{13}$C NMR. The barrier to rotation must be small, as $^1$H NMR experiments performed at −35 °C failed to show any evidence for peak broadening.

Surprisingly, **7** is not soluble in $CD_2Cl_2$ at room temperature, whereas the other ruthenium compounds are. In acetone-$d_6$, the olefinic protons appear upfield at 4.48 ppm, and the two methylene peaks appear at 2.29 and 1.61 ppm. As in **3**, a single

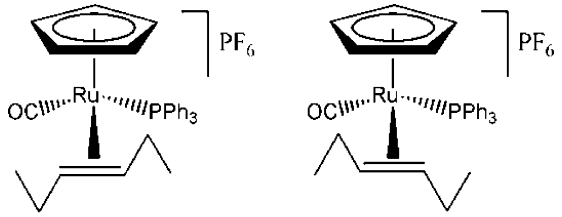


**Figure 5.** Diastereomers of **11**.

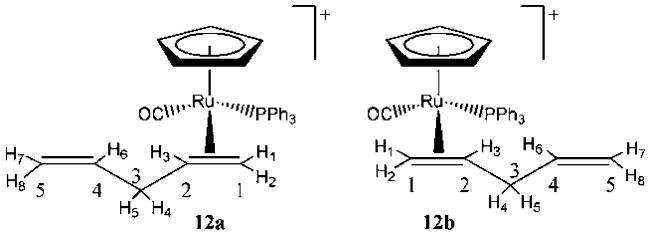


**Figure 6.** Diastereomers of [CpRu(CO)($PPh_3$)(1,4ptd)]$PF_6$ (**12**).

$^1$H NMR methyl signal for the olefin is observed at 1.17 ppm, and the inequivalent CO groups are observed at 201.27 and 196.23 ppm in the $^{13}$C NMR spectrum. These data show that the olefin is rotating rapidly, as in **3**.

At room temperature, the $^1$H NMR spectrum of **11** does not exhibit any distinguishable peaks for the hydrogens on the olefin bond. Broad phenyl peaks are observed downfield at ∼7.50 ppm with a singlet Cp peak appearing at 5.75 ppm. No peaks are observed further upfield, except for a large broad signal at 1.51 ppm. After the NMR tube is cooled to −25 °C, sharp peaks for the olefinic protons are observed at 5.01 and 3.26 ppm. The chemical shifts of these proton resonances are very different from those in **10** at 3.88 and 3.49 ppm. Four distinct methylene resonances are observed at 3.23, 2.38, 1.66, and 1.01 ppm, and two methyl peaks appear at 1.23 and 0.67 ppm. Depending on the face through which the olefin binds to the metal, two isomers (Figure 5) of **11** can form. The ethyl groups on the olefin could point toward the Cp and the CO, as in **11a**, or toward the Cp and the $PPh_3$, as in **11b**. In the X-ray structure of **10**, the ethyl groups of the *cis*-3-hexene both point up and away from the $PPh_3$ ligand. In the case of **11**, one of the ethyl groups will always be directed toward the Cp. The other ethyl group is then either pointing toward the $PPh_3$ or the CO. On the basis of the structure of **10**, it is likely that the ethyl group would point toward the small CO ligand, as in **11a**. The olefin resonance in the $^1$H NMR spectrum of **11** at 3.26 ppm is similar to the signals at 3.88 and 3.49 ppm for the olefin protons in **10** and may therefore be assigned to the olefin proton in **11a** that is pointing away from the Cp ligand. The other olefin proton has a chemical shift (5.01 ppm) that is similar to those in **1** (5.15 ppm) and **2** (5.21 ppm), in which the olefin protons are likely pointing toward the Cp. Isomer **11a** should give rise to four different methylene signals, as previously discussed for **10**. In the $^1$H−$^1$H COSY spectrum of **11** at −25 °C, the peaks at 3.23 and 1.01 ppm are coupled to one another as well as to the olefin peak at 3.26 ppm. These peaks may therefore be assigned to the $CH_2$ protons on the ethyl group that is pointing toward the Cp plane. The remaining methylene proton signals at 2.38 and 1.66 ppm, which are coupled to one another and to the olefin peak at 5.01 ppm, may therefore be assigned to the $CH_2$ group near the CO ligand. The chemical shifts (2.38 and 1.66 ppm) are similar to those (2.12 and 1.83 ppm) of the methylene protons of **10**, providing support for structure **11a** for compound **11**. There is no evidence for isomer **11b**, which means that the formation of **11** is very selective for coordination to one face of the t3hx. The high selectivity of **11** for one face of the *trans*-3-hexene is surprising, as the compounds [CpRe(NO)($PPh_3$)(*trans*-2-butene)]$^+$ (**15**) and [CpRe(NO)($PPh_3$)(*trans*-3-hexene)]$^+$ (**16**) both exhibit lower kinetic selectivity. At room temperature, **15** forms an 85:15 ratio of the *RSS*,*SRR* and *RRR*,*SSS* diastereomers, whereas compound **16** exhibits a lower selectivity ratio of 52:48. When the temperature is increased to 85 °C, equilibrium values of >99:1 are obtained for both **15** and **16**. Thermodynamic equilibrium values for **11** could not be obtained, as the compound begins to degrade at higher temperatures. The selective binding of ruthenium to one face of an olefin has been reported earlier for the series of (Pybox)$RuCl_2$(η²-olefin) complexes by Nishiyama and co-workers.[18]

**[Cp′Ru(CO)(L)(η²-1,4ptd)]Y Complexes (4, 8, and 12).** Although methyl oleate forms the isolable complexes **1**, **5**, and **9**, attempts to prepare analogous complexes with methyl linoleate (*cis*,*cis*-$CH_3(CH_2)_4CH{=}CHCH_2CH{=}CH(CH_2)_7CO_2$Me), containing a 1,4-diene unit, yielded mixtures of oily products that decomposed upon attempted purification. In order to explore the possibility that the 1,4-diene unit in methyl linoleate could bind to metal centers, complexes of 1,4-pentadiene (1,4ptd) were prepared. The complex [CpRu$(CO)_2$(1,4ptd)]$BF_4$ (**4**) was obtained (Scheme 1) by using excess olefin to ensure that only one of the double bonds of the 1,4-pentadiene would bind to the metal, leaving the other double bond uncoordinated. In the $^1$H NMR spectrum of **4**, peaks for the bound olefinic group appear at 5.21, 4.05, and 3.69 ppm, with the last two peaks appearing as doublets due to coupling ($J$ = 8.4 and 14 Hz) with the peak at 5.21 ppm. The magnitudes of the coupling constants indicate that the proton at 4.05 ppm is cis to the proton at 5.21 ppm, while the proton at 3.69 ppm is trans to the proton at 5.21 ppm. As in the complexes of 18:1, c3hx, and t3hx (**1**−**3**, **5**−**7**, **9**−**11**), the internal methylene protons, $H_4$ and $H_5$, appear as two separate multiplets at 3.07 and 2.66 ppm. In the $^{13}$C NMR spectrum, two CO peaks are observed at 195.11 and 194.39 ppm because there is no plane of symmetry in the complex. The unbound olefin carbons ($C_4$ and $C_5$) appear at 135.25 and 119.38 ppm, in contrast to the bound olefin carbons, which appear much further upfield at 84.12 and 51.08 ppm. Low-temperature $^1$H NMR experiments at −35 °C do not result in broadening.

The $^1$H NMR spectrum of **8** exhibits peaks for the bound olefinic group at 4.10, 3.57, and 3.03 ppm with the last two appearing as doublets with coupling constants of 14 and 8.4 Hz, respectively. Unbound olefin resonances appear downfield at 5.98 and 5.29 ppm, and two methylene signals are observed at 3.17 and 2.49 ppm. Unlike compounds **1**−**7** and **9**−**12**, **8** decomposes rapidly in solution and even slowly in the solid state. The decomposition appears to yield a discrete product with new peaks appearing at 4.38, 3.67, 3.45, and 2.85 ppm. An off-white compound with essentially the same $^1$H NMR spectrum was obtained when 2 equiv of Cp*$Ru(CO)_2Cl$ was reacted with 1 equiv of 1,4-pentadiene in the presence of $AgPF_6$. Therefore, the product of the decomposition of **8** was assigned the structure [Cp*$Ru(CO)_2]_2$(1,4ptd)$^{2+}$, in which a [Cp*Ru$(CO)_2]^+$ unit is coordinated to each double bond of the 1,4ptd ligand. It should be noted that we previously reported the isolation and X-ray characterization of the complex [CpPd$(PMe_3)]_2$(1,4ptd)$^{2+}$, in which a [CpPd$(PMe_3)]^+$ unit was coordinated to each of the double bonds in the 1,4ptd.[9]

(18) Motoyama, Y.; Murata, K.; Kurihara, O.; Naitoh, T.; Aoki, K.; Nishiyama, H. *Organometallics* **1998**, *17*, 1251.

**Table 2. Rate Constants for the Reaction (Eq 1) of $[Cp'Ru(CO)_2(olefin)]^+$ with $PPh_3$ in $CDCl_3$ at 40.0 °C**

| compd | $10^6k_1$, $s^{-1}$ | $10^5k_2$, $M^{-1}$ $s^{-1}$ |
|---|---|---|
| $CpRu(CO)_2(18:1)^+$ (**1**) | 1.28 | 6.08 |
| $CpRu(CO)_2(c3hx)^+$ (**2**) | 1.96 | 6.08 |
| $Cp^*Ru(CO)_2(c3hx)^+$ (**6**) | 21.8 | 3.04 |
| $Cp^*Ru(CO)_2(t3hx)^+$ (**7**) | 208 | 0.0 |

Due to the asymmetry of the $[CpRu(CO)(PPh_3)]^+$ fragment, **12** exists as the two diastereomers **12a** and **12b** (Figure 6), depending on the face of the olefin to which the metal is coordinated. Peak assignments were made on the basis of $^1H-^1H$ COSY and $^1H-^{13}C$ HETCOR experiments as well as peak integrations. The diastereomers were differentiated by the chemical shifts of $H_2$, which can either be opposite the $PPh_3$ ligand, as in **12a**, or the CO ligand, as in **12b**. The $H_2$ peak of the major isomer occurs at 4.06 ppm, whereas the peak of the minor isomer occurs at 3.59 ppm. The more upfield peak at 3.59 ppm is assigned to $H_2$ situated near the $PPh_3$ ligand. Thus, the major isomer with the more downfield 4.06 ppm value for $H_2$ is assigned structure **12a**, in which the free olefin is situated near the CO ligand; the minor diastereomer, **12b**, has the free olefin opposite the $PPh_3$. Isolated complex **12** contains a 1.00:0.65 ratio of **12a** and **12b**; due to the slow rate of olefin dissociation (see below) it seems likely that the diastereomers are not in equilibrium. During the formation of **12**, **12a** would likely be the preferred structure, due to reduced steric interactions between the bulky $PPh_3$ ligand and the unbound olefinic group. Unfortunately, the compound decomposes upon heating to 50 °C in $CD_2Cl_2$, so that thermodynamic equilibrium ratios could not be determined. The internal methylene in **12a** at 2.70 ppm exists as a multiplet, whereas the methylene splitting is larger in the minor isomer, with peaks appearing at 2.65 and 1.94 ppm, which may be due to greater shielding of one of the methylene protons by the $PPh_3$ ligand. The presence of the two isomers is also evident in the $^{31}P$ NMR spectrum of **12**, which shows a phosphine peak for **12a** at 50.36 ppm and for **12b** at 49.05 ppm. No noticeable broadening or changes in chemical shifts were observed in the $^1H$ NMR spectrum of a sample of **12** at −35 °C.

**Kinetic Studies of Olefin Substitution in the $[Cp'Ru(CO)_2(\eta^2\text{-olefin})]^+$ Complexes.** The $[Cp'Ru(CO)_2(\eta^2\text{-olefin})]^+$ complexes react (eq 1) with $PPh_3$ to give the free olefin and the $[Cp'Ru(CO)_2(PPh_3)]^+$ complexes. Kinetic studies of this reaction

$$[Cp'Ru(CO)_2(olefin)]BF_4 + PPh_3 \rightarrow [Cp'Ru(CO)_2(PPh_3)]BF_4 + olefin \quad (1)$$

at 40.0 °C in $CDCl_3$ solvent were performed under pseudo-first-order conditions with at least a 10-fold excess of $PPh_3$. The compounds used in the kinetic studies were **1**, **2**, **6**, and **7**. Unfortunately, the other complexes did not give useful kinetic results for various reasons, including low solubility (**3**), decomposition (**4**, **8**, **9**−**12**), and weighing problems due to oily composition (**5**). The $k_{obs}$ values (see Table S1 in the Supporting Information) obtained from slopes of first-order plots depend upon the $PPh_3$ concentration in the following way: $k_{obs} = k_1 + k_2[PPh_3]$. For complex **7**, the $k_2$ term is negligible, so that $k_{obs} = k_1$. Rate constant values for each complex are given in Table 2. The $PPh_3$-independent term ($k_1$) is consistent with a mechanism in which the rate-determining step is the dissociation of the olefin ligand. The $PPh_3$-dependent term ($k_2$) is consistent with an associative mechanism involving rate-determining addition of $PPh_3$ to the complex.

Since the $k_1$ values describe the rate of olefin dissociation, it is expected that these values will reflect the strength of the Ru−olefin bond or the stability of the transition state. A comparison of $k_1$ values for complexes **1** and **2** shows that c3hx dissociates slightly faster than 18:1, but the difference between them is small. Thus, the long and short alkyl groups on the cis olefinic bond do not greatly affect the rate of the olefin dissociation. In equilibrium studies[9] of the substitution of the NCR′ ligand in $[CpPd(PR_3)(NCR')]^+$ by olefins, it was observed that $K$ values for 18:1 were only a factor of 2 less than those for c3hx. Thus, in both the kinetic and equilibrium studies, the length of the alkyl groups on the cis olefin exerts a relatively small influence on olefin binding to the metal.

In contrast to the very similar values for complexes **1** and **2**, the rate of c3hx dissociation from $[Cp^*Ru(CO)_2(c3hx)]^+$ (**6**) is approximately 10 times faster than from $[CpRu(CO)_2(c3hx)]^+$ (**2**). Similarly, the dissociative pathway ($k_1$) for the substitution of the dibenzothiophene (DBT) in $[Cp^*Ru(CO)_2(DBT)]^+$ by phosphines is 29 times faster than that for the dissociation of DBT from the Cp analogue, $[CpRu(CO)_2(DBT)]^+$.[19] The large difference in rates between **2** and **6** may be attributed to steric repulsions between the c3hx and Cp* ligands in **6** being greater than those between c3hx and Cp ligands in **2**. Alternatively, the Cp* ligand may better stabilize the electron-deficient metal as the olefin dissociates. A comparison of $k_1$ values for **6** and **7** shows that t3hx dissociates nearly 10 times faster than c3hx from $[Cp^*Ru(CO)_2]^+$. This difference in rates may be attributed to the much smaller steric effect of the ethyl groups, which may be directed away from the bulky Cp* ligand in **6**, while an ethyl group in the t3hx ligand is forced to interact with the Cp* in all orientations of the t3hx ligand in **7** (Figure 1). Equilibrium studies of the binding of cis and trans olefins to Ag(I), Cu(I), Rh(I), and Pt(II) also show that cis olefins generally coordinate more strongly than trans olefins.[20]

Observation of the same $k_2$ values (Table 2) for compounds **1** and **2** is surprising, because a pathway involving nucleophilic attack of $PPh_3$ on the Ru should be slower for the larger 18:1 than for c3hx. The same rates for these reactions could mean that either the $PPh_3$ attack is from a side of the Ru away from the olefin or the rate of this associative pathway is dominated by breaking of the Ru−olefin bond rather than making of the Ru−$PPh_3$ bond. The similar $k_1$ values for **1** and **2** suggest that the strengths of the Ru−olefin bonds in these compounds are similar.

A comparison of $k_2$ values for **2** and **6** shows that $k_2$ is slightly smaller for the Cp* complex (**6**). Because the $k_1$ values indicate that the c3hx is less strongly bound in **6** than in **2**, the slower rate of c3hx substitution in **6** is probably due to the bulky Cp*, which reduces the rate of $PPh_3$ addition to **6** as compared with that to **2**. In the case of compound **7**, the $k_1$ value is so large that it is not possible to measure a $k_2$ value for this compound, which indicates that t3hx dissociates so rapidly by the $k_1$ pathway that an associative pathway is not competitive.

## Conclusions

The series of complexes $[Cp'Ru(CO)(L)(\eta^2\text{-olefin})]^+$ (Cp′ = Cp, Cp*; L = CO, $PPh_3$, olefin = 18:1, c3hx, t3hx, 1,4ptd) were prepared and characterized by their IR and $^1H$, $^{13}C\{^1H\}$,

(19) Vecchi, P. A.; Ellern, A.; Angelici, R. J. *Organometallics* **2005**, *24*, 2168.

(20) (a) Blytas, G. C. In *Separation and Purification Technology*; Li, N. N., Calo, J. M., Eds.; Marcel Dekker: New York, 1992. (b) Hughes, R. P. In *Comprehensive Organometallic Chemistry*; Wilkinson, G., Stone, F. G. A., Abel, E. W., Eds.; Pergamon Press: Oxford, England, 1982; Vol. 5. (c) Young, G. B. *Comprehensive Organometallic Chemistry*; Wilkinson, G., Stone, F. G. A., Abel, E. W., Puddephatt, R. J., Eds.; Pergamon Press: Oxford, England, 1995; Vol. 9.

and $^{31}P\{^{1}H\}$ NMR spectra. An X-ray structural study of **10** shows that the C═C bond of the olefin is approximately parallel to the plane of the Cp ligand. Only for $[CpRu(CO)(PPh_3)(\eta^2\text{-t3hx})]^+$ (**11**) was it possible to show conclusively that the olefin ligand rotates slowly on the NMR time scale (at −25 °C). The preparation of **11** gives only one diastereomer, demonstrating that the $[CpRu(CO)(PPh_3)]^+$ unit is highly selective for coordination to one face of the olefin. The synthesis of $[CpRu(CO)(PPh_3)(\eta^2\text{-1,4ptd})]^+$ gives a 1.0:0.65 ratio of the two possible diastereomers. Selective binding of one face of an olefin to metal complexes is important in catalytic reactions involving stereocenters, as in olefin polymerization catalyzed by $R_2TiCl_2$ compounds,[21] enantioselective diboration of alkenes by $L_nM(BR_2)_2$,[22] and ring-closing olefin metathesis.[23] Kinetic studies of olefin substitution in the $[Cp'Ru(CO)_2(\eta^2\text{-olefin})]^+$ complexes show that the rate of olefin dissociation is (1) very similar for c3hx and 18:1, (2) much faster when Cp′ is Cp* rather than Cp, and (3) much faster for t3hx than for c3hx. The difference between the reactions of $[CpRu(CO)_2(c3hx)]^+$ (**2**) and $[CpFe(CO)_2(\eta^2\text{-}H_2C{=}CH_2)]^+$ with $PPh_3$ is worth noting. While the $PPh_3$ simply replaces the c3hx ligand in **2**, the $PPh_3$ adds to the ethylene in the Fe complex to give $[CpFe(CO)_2(CH_2CH_2PPh_3)]^+$.[24] Steric and electronic differences between ethylene and c3hx may account for this difference, because $[CpRu(CO)_2(\eta^2\text{-}H_2C{=}CH_2)]^+$ also undergoes attack at the ethylene when reacted with $NH_3$.[25]

## Experimental Section

**Methods and Materials**. All reactions were carried out under an inert atmosphere of dry argon using standard Schlenk techniques. Diethyl ether, methylene chloride, and hexanes were purified on alumina using a Solv-Tek solvent purification system, similar to that reported by Grubbs.[26] The olefins methyl oleate (18:1), methyl linoleate (18:2), *trans*-3-hexene (t3hx), 1,4-pentadiene (1,4ptd), and styrene were purchased from Sigma-Aldrich Chemical Co. and used as received. *cis*-3-Hexene (c3hx) was purchased from TCI Chemical Co. and used as received. All deuterated solvents were purchased from Cambridge Isotope Laboratories. Solution infrared spectra were recorded on a Nicolet-560 spectrophotometer using NaCl cells with a 0.1 mm path length. $^{1}H$, $^{13}C$, and $^{31}P$ NMR spectra were recorded on a Bruker DRX-400 spectrometer using the deuterated solvents as internal references. Elemental analyses were performed on a Perkin-Elmer 2400 Series II CHNS/O analyzer. The compounds $CpRu(CO)_2Cl$,[27] $Cp^*Ru(CO)_2Cl$,[28] and $CpRu(CO)(PPh_3)Cl$[29] were all prepared according to reported methods.

**General Procedure for Preparations of the $[CpRu(CO)_2(\eta^2\text{-olefin})]BF_4$ Complexes (1−4)**. To a mixture of dry $CH_2Cl_2$ (20 mL) containing $AgBF_4$ (75.6 mg, 0.388 mmol) was added $CpRu(CO)_2Cl$ (100 mg, 0.388 mmol) and 1.2 mmol of olefin (olefin = 18:1, c3hx, t3hx, 1,4ptd). The solution was stirred at room temperature for 4−6 h until the reaction was complete, as indicated by the IR spectrum. The solution was then filtered to remove AgCl and concentrated in vacuo to approximately 1 mL, and then 20 mL of hexanes was added to precipitate the product. The tan solid products were isolated by filtration and washed with hexanes (3 × 5 mL) to remove excess olefin. Isolated yields were typically 75−85%. The products could be further purified by recrystallization from $CH_2Cl_2$/ether. The $^{1}H$ NMR and $^{13}C$ NMR spectra were obtained in either $CDCl_3$ or $CD_2Cl_2$, depending on the compound solubility.

**Characterization of Compounds 1−4. $[CpRu(CO)_2(\eta^2\text{-18:1})]BF_4$ (1).** $^{1}H$ NMR ($CDCl_3$, 400 MHz, 293 K): $\delta$ 5.89 (s, 5H, $C_5H_5$), 5.15 (m, 2H, $H_{9,10}$), 3.66 (s, 3H, OMe), 2.31 (t, $^{3}J_{HH}$ = 7.2 Hz, 3H, $H_2$), 2.19 (m, 2H, $H_{8,11}$), 1.97 (m, 2H, $H_{8,11}$), 1.27−1.65 (m, 22 H, $H_{3,12}$), 0.90 (t, $^{3}J_{HH}$ = 6.4 Hz, 3H, $H_{18}$). $^{13}C\{^{1}H\}$ NMR ($CDCl_3$, 100 MHz, 293 K): $\delta$ 195.15, 195.08 (C≡O), 174.47 (C═O), 91.21 ($C_5H_5$), 81.04 ($C_{10}$), 80.88 ($C_9$), 51.04 (OMe), 34.20 ($C_2$), 32.00−22.86 ($C_{3,8,11,12}$), 14.31 ($C_{18}$). IR ($CH_2Cl_2$; $cm^{-1}$): $\nu$(CO) 2076 (s), 2032 (s); $\nu$(C═O) 1731 (s). Anal. Calcd for $C_{26}H_{41}BF_4O_4Ru$: C, 51.58; H, 6.83. Found: C, 51.09; H, 6.77.

**$[CpRu(CO)_2(\eta^2\text{-c3hx})]BF_4$ (2).** $^{1}H$ NMR ($CDCl_3$, 400 MHz, 293 K): $\delta$ 5.91 (s, 5H, $C_5H_5$), 5.21 (m, 2H, $H_{3,4}$), 2.28 (m, 2H, $H_{2,5}$), 2.08 (m, 2H, $H_{2,5}$), 1.25 (t, $^{3}J_{HH}$ = 7.2 Hz, 6H, $H_{1,6}$). $^{13}C\{^{1}H\}$ NMR ($CDCl_3$, 100 MHz, 293 K): $\delta$ 194.85 (C≡O), 90.98 ($C_5H_5$), 82.15 ($C_{3,4}$), 24.56 ($C_{2,5}$), 15.55 ($C_{1,6}$). IR ($CH_2Cl_2$; $cm^{-1}$): $\nu$(CO) 2077 (s), 2033 (s). Anal. Calcd for $C_{13}H_{17}BF_4O_2Ru$: C, 39.71; H, 4.37. Found: C, 39.69; H, 4.46.

**$[CpRu(CO)_2(\eta^2\text{-t3hx})]BF_4$ (3).** $^{1}H$ NMR ($CD_2Cl_2$, 400 MHz, 293 K): $\delta$ 5.87 (s, 5H, $C_5H_5$), 4.86 (m, 2H, $H_{3,4}$), 2.23 (m, 2H, $H_{2,5}$), 1.64 (m, 2H, $H_{2,5}$), 1.17 (t, $^{3}J_{HH}$ = 7.6 Hz, 6H, $H_{1,6}$). $^{13}C\{^{1}H\}$ NMR (acetone-$d_6$, 100 MHz, 293 K): $\delta$ 197.02 (C≡O), 192.58 (C═O), 91.78 ($C_5H_5$), 85.15 ($C_{3,4}$), 32.89 ($C_{2,5}$), 18.12 ($C_{1,6}$). IR ($CH_2Cl_2$; $cm^{-1}$): $\nu$(CO) 2078 (s), 2035 (s). Anal. Calcd for $C_{13}H_{17}BF_4O_2Ru$: C, 39.71; H, 4.37. Found: C, 40.07; H, 4.77.

**$[CpRu(CO)_2(\eta^2\text{-1,4ptd})]BF_4$ (4).** $^{1}H$ NMR ($CD_2Cl_2$, 400 MHz, 293 K): $\delta$ 5.89 (s, 5H, $C_5H_5$), 5.82 (m, 1H, $H_4$), 5.21 (m, 3H, $H_{2,5}$), 4.05 (d, $^{3}J_{HH}$ = 8.4 Hz, 1H, $H_1$), 3.69 (d, $^{3}J_{HH}$ = 14 Hz, 1H, $H_1$), 3.07 (m, 1H, $H_4$ or $H_5$), 2.66 (m, 1H, $H_4$ or $H_5$). $^{13}C\{^{1}H\}$ NMR ($CD_2Cl_2$, 100 MHz, 293 K): $\delta$ 195.11 (C≡O), 194.39 (C≡O), 135.25 ($C_4$), 119.38 ($C_5$), 91.63 ($C_5H_5$), 84.12 ($C_2$), 51.08 ($C_1$), 40.60 ($C_3$). IR ($CH_2Cl_2$; $cm^{-1}$): $\nu$(CO) 2083 (s), 2040 (s). Anal. Calcd for $C_{12}H_{13}BF_4O_2Ru$: C, 38.21; H, 3.48. Found: C, 37.89; H, 3.32.

**General Procedure for Preparations of the $[Cp^*Ru(CO)_2(\eta^2\text{-olefin})]PF_6$ Complexes (5−8)**. To a solution of dry $CH_2Cl_2$ (20 mL) containing $AgPF_6$ (77.1 mg, 0.305 mmol) was added $Cp^*Ru(CO)_2Cl$ (100 mg, 0.305 mmol) and 0.915 mmol of olefin (olefin = 18:1, c3hx, t3hx, 1,4ptd). The solution was stirred for 4 h at room temperature until the reaction was complete, as indicated by the IR spectrum. The solution, which contained AgCl precipitate, was then filtered and concentrated in vacuo. Because the 18:1 salt does not precipitate when hexane is added, the product could only be partially purified by repeated washing with hexane to remove unbound methyl oleate. The other olefin salts (**6**−**8**) were easily precipitated by hexane, filtered, and washed with additional hexane (3 × 5 mL). The 18:1 salt (**5**) was obtained as a dark brown oil, whereas the other salts were obtained as light tan solids. Isolated yields were typically 55−80%. The solid products could be recrystallized from $CH_2Cl_2$/ether. Depending on their solubilities, $^{1}H$ NMR and $^{13}C$ NMR spectra of the compounds were taken in $CDCl_3$, $CD_2Cl_2$, or acetone-$d_6$.

**Characterization of Compounds 5−8. $[Cp^*Ru(CO)_2(\eta^2\text{-18:1})]PF_6$ (5).** $^{1}H$ NMR ($CDCl_3$, 400 MHz, 293 K): $\delta$ 3.88 (m, 2H, $H_{9,10}$), 3.65 (s, 3H, OMe), 2.30 (t, $^{3}J_{HH}$ = 7.6 Hz, 2H, $H_2$), 2.10 (m, 2H $H_{8,11}$), 1.98 (s, 15H, $C_5Me_5$), 1.95 (m, 2H, $H_{8,11}$), 1.20−1.65 (m, 22H, $H_{3,12}$), 0.872 (t, $^{3}J_{HH}$ = 6.8 Hz, 3H, $CH_3$). $^{13}C\{^{1}H\}$

(21) Eisch, J. J.; Gitua, J. N. *Organometallics* **2003**, *22*, 4172.
(22) Trudeau, S.; Morgan, J. B.; Shrestha, M.; Morken, J. P. *J. Org. Chem.* **2005**, *70*, 9538.
(23) Funk, T. W.; Berlin, J. M.; Grubbs, R. H. *J. Am. Chem. Soc.* **2006**, *128*, 1840.
(24) (a) Rosan, A.; Rosenblum, M.; Tancrede, J. *J. Am. Chem. Soc.* **1973**, *95*, 3062. (b) Nicholas, K. M.; Rosan, A. M. *J. Organomet. Chem.* **1975**, *84*, 351.
(25) Behrens, H.; Jungbauer, A. *Z. Naturforsch., B* **1979**, *34*, 1477.
(26) Pangborn, A. B.; Giardello, M. A.; Grubbs, R. H.; Rosen, R. K.; Timmers, F. J. *Organometallics* **1996**, *15*, 1518.
(27) Eisenstadt, A.; Tannenbaum, R.; Efraty, A. *J. Organomet. Chem.* **1981**, *221*, 317.
(28) Nagashima, H.; Mukai, K.; Shiota, Y.; Yamaguchi, K.; Ara, K.; Fukahori, T.; Suzuki, H.; Akita, M.; Moro-oka, Y.; Itoh, K. *Organometallics* **1990**, *9*, 799.
(29) Davies, S. G.; Simpson, S. J. *J. Chem. Soc., Dalton Trans.* **1984**, 993.

NMR ($CDCl_3$, 100 MHz, 293 K): $\delta$ 198.51 (C≡O), 198.47 (C≡O), 174.43 (C═O), 104.39 ($C_5Me_5$), 84.14 ($C_{10}$), 83.99 ($C_9$), 51.64 (OMe), 34.14 ($C_2$), 31.93−22.80 ($C_{3,8,11,12}$), 14.25 ($C_{18}$), 9.74 ($C_5Me_5$). IR ($CH_2Cl_2$; $cm^{-1}$): $\nu$(CO) 2061 (s), 2016 (s); $\nu$(C═O) 1732 (s).

**[Cp*Ru(CO)$_2$($\eta^2$-c3hx)]PF$_6$ (6).** $^1$H NMR ($CD_2Cl_2$, 400 MHz, 293 K): $\delta$ 3.86 (m, 2H, $H_{3,4}$), 2.20 (m, 2H, $H_{2,5}$), 2.12 (m, 2H, $H_{2,5}$), 2.02 (s, 15 H, $C_5Me_5$), 1.22 (t, $^3J_{HH}$ = 7.2 Hz, 6 H, $H_{1,6}$). $^{13}C\{^1H\}$ NMR ($CD_2Cl_2$, 100 MHz, 293 K): $\delta$ 198.62 (C≡O), 104.63 ($C_5Me_5$), 86.02 ($C_{3,4}$), 25.09 ($C_{2,5}$), 15.98 ($C_{1,6}$), 10.12 ($C_5Me_5$). IR ($CH_2Cl_2$; $cm^{-1}$): $\nu$(CO) 2062 (s), 2018 (s). Anal. Calcd for $C_{18}H_{27}PF_6O_2Ru$: C, 41.45; H, 5.23. Found: C, 41.58; H, 5.39.

**[Cp*Ru(CO)$_2$($\eta^2$-t3hx)]PF$_6$ (7).** $^1$H NMR (acetone-$d_6$, 400 MHz, 293 K): $\delta$ 4.48 (m, 2H, $H_{3,4}$), 2.29 (m, 2H, $H_{2,5}$), 2.15 (s, 15H, $C_5Me_5$), 1.61 (m, 2H, $H_{2,5}$), 1.17 (t, $^3J_{HH}$ = 7.2 Hz, 6H, $H_{1,6}$). $^{13}C$ NMR (acetone-$d_6$, 400 MHz, 293 K): $\delta$ 201.27 (C≡O), 196.23 (C≡O), 105.393 ($C_5Me_5$), 88.75 ($C_{3,4}$), 31.32 ($C_{2,5}$), 18.51 ($C_{1,6}$), 10.23 ($C_5Me_5$). IR ($CH_2Cl_2$; $cm^{-1}$): $\nu$(CO) 2063 (s), 2020 (s).

**[Cp*Ru(CO)$_2$($\eta^2$-1,4ptd)]PF$_6$ (8).** $^1$H NMR ($CD_2Cl_2$, 400 MHz, 293 K): $\delta$ 5.98 (m, 1H, $H_4$), 5.29 (m, 2H, $H_5$), 4.10 (m, 1H, $H_2$), 3.57 (d, $^3J_{HH}$ = 14 Hz, 1H, $H_1$), 3.17 (m, 1H, $H_3$), 3.03 (d, $^3J_{HH}$ = 8.4 Hz, 1 H, $H_1$), 2.49 (m, 1 H, $H_3$), 2.02 (s, 15 H, $C_5Me_5$). $^{13}C$ NMR ($CD_2Cl_2$, 100 MHz, 293 K): $\delta$ 198.21 (C≡O), 197.42 (C≡O), 134.80 ($C_4$), 118.02 ($C_5$), 104.83 ($C_5Me_5$), 85.12 ($C_2$), 56.38 ($C_1$), 40.09 ($C_3$), 9.98 ($C_5Me_5$). IR ($CH_2Cl_2$; $cm^{-1}$): $\nu$(CO) 2069 (s), 2026 (s).

**General Procedure for Preparations of the [CpRu(CO)(PPh$_3$)($\eta^2$-olefin)]PF$_6$ Complexes (9−12)**. To a solution of dry $CH_2Cl_2$ (20 mL) containing $AgPF_6$ (51.4 mg, 0.203 mmol) was added CpRu(CO)($PPh_3$)Cl (100 mg, 0.203 mmol) and 0.610 mmol of olefin (olefin = 18:1, c3hx, t3hx, 1,4ptd). The solution was stirred at room temperature for 4−6 h until the reaction was complete according to the IR spectrum. The solution was then filtered to remove the AgCl precipitate and concentrated in vacuo. Because the 18:1 salt does not precipitate when hexane is added, the product could only be partially purified by repeated washing with hexane to remove unbound methyl oleate. The other olefin salts were easily precipitated by hexane, filtered, and washed with additional hexane (3 × 5 mL). The 18:1 salt (**9**) was obtained as a viscous yellow oil, whereas the other salts were obtained as light yellow solids. Isolated yields were typically 70−80%. The solid products could be recrystallized from $CH_2Cl_2$/ether. Depending on their solubilities, $^1$H NMR and $^{13}C$ NMR spectra of the compounds were taken in either $CDCl_3$, $CD_2Cl_2$, or acetone-$d_6$.

**Characterization of Compounds 9−12**. **[CpRu(CO)(PPh$_3$)($\eta^2$-18:1)]PF$_6$ (9).** $^1$H NMR ($CDCl_3$, 400 MHz, 293 K): $\delta$ 7.65 (m, 9H, $Ph_{m,p}$), 7.16 (m, 6H, $Ph_o$), 5.20 (s, 5H, $C_5H_5$), 3.80 (m, 1H, $H_{10}$), 3.66 (s, 3H, OMe), 3.48 (m, 1H, $H_9$), 2.30 (t, $^3J_{HH}$ = 7.8 Hz, 2H, $H_2$), 2.01 (m, 2H, $H_{11}$), 1.77 (m, 2H, $H_8$), 0.95−1.65 (m, 22H, $H_{3,12}$), 0.87 (t, $^3J_{HH}$ = 6.4 Hz, 3H, $H_{18}$). $^{13}C\{^1H\}$ NMR ($CDCl_3$, 100 MHz, 293 K): $\delta$ 204.27 (d, $^2J_{PC}$ = 20.0 Hz, C≡O), 174.45 (C═O), 132.65 (d, $^2J_{PC}$ = 10.2 Hz, $C_o$), 132.11 (d, $^4J_{PC}$ = 2.0 Hz, $C_p$), 130.02 (d, $^1J_{PC}$ = 24.1 Hz, $C_i$), 129.70 (d, $^3J_{PC}$ = 10.6, $C_m$), 91.68 ($C_5H_5$), 77.11 ($C_{10}$), 75.50 ($C_9$), 51.58 (OMe), 34.14 ($C_2$), 33.29−22.80 ($C_{3,8,11,12}$), 14.27 ($C_{18}$). IR ($CH_2Cl_2$; $cm^{-1}$): $\nu$(CO) 2003 (s); $\nu$(C═O) 1732 (s).

**[CpRu(CO)(PPh$_3$)($\eta^2$-c3hx)]PF$_6$ (10).** $^1$H NMR ($CD_2Cl_2$, 400 MHz, 293 K): $\delta$ 7.57 (m, 9H, $Ph_{m,p}$), 7.21 (m, 6H, $Ph_o$), 5.21 (s, 5H, $C_5H_5$), 3.88 (m, 1H, $H_3$), 3.49 (m, 1H, $H_4$), 2.12 (m, 2H, $H_2$), 1.83 (m, 2H, $H_5$), 1.23 (t, $^3J_{HH}$ = 7.2 Hz, 3H, $H_1$), 0.88 (t, $^3J_{HH}$ = 3.6 Hz, 3H, $H_6$). $^{13}C\{^1H\}$ NMR ($CD_2Cl_2$, 100 MHz, 293 K): $\delta$ 204.75 (d, $^2J_{CP}$ = 19.9 Hz, C≡O), 133.04 (d, $^2J_{CP}$ = 10.2 Hz, $C_o$), 132.58 (d, $^4J_{CP}$ = 2.4 Hz, $C_p$), 130.13 ($C_i$), 130.02 ($C_m$), 91.91 (d, $^1J_{CP}$ = 1.4 Hz, $C_5H_5$), 79.63 ($C_3$), 77.43 ($C_4$), 26.85 ($C_2$), 26.69 ($C_5$), 17.60 ($C_1$), 16.67 ($C_6$). $^{31}P\{^1H\}$ NMR ($CD_2Cl_2$, 162 MHz, 293 K): $\delta$ 48.50 (s). IR ($CH_2Cl_2$; $cm^{-1}$): $\nu$(CO) 2000 (s). Anal. Calcd for $C_{30}H_{32}F_6OP_2Ru$: C, 52.56; H, 4.70. Found: C, 52.79; H, 4.72.

**[CpRu(CO)(PPh$_3$)($\eta^2$-t3hx)]PF$_6$ (11).** $^1$H NMR (acetone-$d_6$, 400 MHz, 250 K): $\delta$ 7.65 (m, 9H, $Ph_{m,p}$), 7.43 (m, 6H, $Ph_o$), 5.75 (s, 5H, $C_5H_5$), 5.01 (m, 1H, $H_3$), 3.26 (m, 1H, $H_4$), 3.23 (m, 1H, $H_5$), 2.38 (m, 1H, $H_2$), 1.66 (m, 1H, $H_2$), 1.23 (t, $^3J_{HH}$ = 7.2 Hz, 3H, $H_1$), 1.01 (m, 1H, $H_5$), 0.67 (t, $^3J_{HH}$ = 7.2 Hz, 3H, $H_6$). $^{13}C\{^1H\}$ NMR (acetone-$d_6$, 100 MHz, 250 K): $\delta$ 203.96 (C≡O), 133.92 ($C_o$), 132.39 ($C_p$), 130.19 ($C_i$), 130.08 ($C_m$), 92.97 ($C_5H_5$), 74.66 ($C_4$), 71.19 ($C_3$), 31.19 ($C_5$), 30.92 ($C_2$), 19.31 ($C_6$), 18.62 ($C_1$). $^{31}P\{^1H\}$ NMR (acetone-$d_6$, 162 MHz, 250 K): $\delta$ 49.52 ($PPh_3$). IR ($CH_2Cl_2$; $cm^{-1}$): $\nu$(CO) 2000 (s). Anal. Calcd for $C_{30}H_{32}F_6OP_2Ru$: C, 52.56; H, 4.70. Found: C, 52.79; H, 4.72.

**Synthesis of [CpRu(CO)(PPh$_3$)($\eta^2$-14ptd)]PF$_6$ (12).** Major isomer (**12a**): $^1$H NMR ($CDCl_3$, 400 MHz, 293 K) $\delta$ 5.89 (m, 1H, $H_6$), 5.36 (s, 5H, $C_5H_5$), 5.14 (m, 2H, $H_{7,8}$), 4.06 (d, $^3J_{HH}$ = 13.6 Hz, 1H, $H_2$), 3.74 (m, 1H, $H_3$), 2.70 (m, 2H, $H_{4,5}$), 2.60 (d, $^3J_{HH}$ = 8.4 Hz, 1H, $H_1$); $^{13}C\{^1H\}$ NMR (acetone-$d_6$, 100 MHz, 293 K) $\delta$ 205.32 (d, $^2J_{CP}$ = 19.0 Hz, C≡O), 138.50 ($C_2$), 134.17 (d, $^3J_{CP}$ = 10.3 Hz, $C_o$), 133.33 (d, $^1J_{CP}$ = 52.6 Hz, $C_i$), 132.87 (d, $^5J_{CP}$ = 2.7 Hz, $C_p$), 130.34 (d, $^4J_{CP}$ = 2.6 Hz, $C_m$), 117.06 ($C_1$), 92.06 (d, $^1J_{CP}$ = 1.1 Hz, $C_5Me_5$), 78.95 ($C_4$), 49.22 ($C_5$), 42.94 ($C_3$); $^{31}P\{^1H\}$ NMR ($CD_2Cl_2$, 162 MHz, 293 K) $\delta$ 50.36 ($PPh_3$). Minor isomer (**12b**): $^1$H NMR ($CDCl_3$, 400 MHz, 293 K) $\delta$ 5.72 (m, 1H, $H_6$), 5.32 (s, 5H, $C_5H_5$), 5.02 (d, $^3J_{HH}$ = 10.4 Hz, 1H, $H_7$), 4.95 (d, $^3J_{HH}$ = 16.8 Hz, 1H, $H_8$), 4.69 (m, 1H, $H_3$), 3.59 (d, $^3J_{HH}$ = 8.4 Hz, 1H, $H_2$), 2.65 (m, 1H, $H_4$), 2.58 (d, $^3J_{HH}$ = 8 Hz, 1H, $H_1$), 1.94 (m, 1H, $H_5$); $^{13}C\{^1H\}$ NMR (acetone-$d_6$, 100 MHz, 293 K) $\delta$ 204.13 (d, $^2J_{CP}$ = 19.7 Hz, C≡O), 139.06 ($C_4$), 133.93 (d, $^3J_{CP}$ = 10.5 Hz, $C_o$), 132.80 (d, $^5J_{CP}$ = 2.4 Hz, $C_p$), 132.08 (d, $^1J_{CP}$ = 52.5 Hz, $C_i$), 130.45 (d, $^4J_{CP}$ = 2.3 Hz, $C_m$), 116.82 ($C_5$), 92.59 ($C_5Me_5$), 70.71 ($C_2$), 48.64 ($C_1$), 40.90 ($C_3$); $^{31}P\{^1H\}$ NMR ($CD_2Cl_2$, 162 MHz, 293 K) $\delta$ 49.05 ($PPh_3$); IR ($CH_2Cl_2$; $cm^{-1}$) $\nu$(CO) 2006 (s). Anal. Calcd for $C_{29}H_{28}F_6OP_2Ru$: C, 52.02; H, 4.22. Found: C, 51.70; H, 4.26.

**General Procedure for Kinetic Studies.** A 0.010 mmol sample of the complex was placed in an NMR tube with an excess, weighed amount of $PPh_3$. The tube was evacuated, flushed with nitrogen, and capped with a septum. A 0.70 mL aliquot of $CDCl_3$ or $CD_2Cl_2$ was added, and the tube was placed in liquid nitrogen. The tube was then flame-sealed under vacuum. After the solution thawed, the tube was placed in a constant-temperature bath at 40.0 ± 0.1 °C. The tube was removed from the bath periodically, and the spectrum was recorded on a Bruker DRX-400 spectrometer at room temperature using the deuterated solvent as the internal lock and standard. The tube was then returned to the bath within a 10 min period. The products formed during the course of the kinetic reactions were $[Cp'Ru(CO)_2(PPh_3)]^+$ [7a,30] and the free olefins, which were identified by their $^1$H NMR spectra. The Cp′ or olefin methyl peaks were integrated using XWIN-NMR software. Rate constants, $k_{obs}$, were obtained from the slopes of first-order least-squares plots of ln (1 + [product]/[reactant]) vs time.[19]

**X-ray Structure Determination of 10.** The crystal evaluations and data collections were performed at 203 K on a Bruker CCD-1000 diffractometer with Mo Kα ($\lambda$ = 0.710 73 Å) radiation and a detector-to-crystal distance of 5.03 cm. The data were collected using the full-sphere routine and were corrected for Lorentz and polarization effects. The absorption correction was based on fitting a function to the empirical transmission surface, as sampled by multiple equivalent measurements using SADABS software. The

(30) Bruce, M. I.; Zaitseva, N. N.; Skelton, B. W.; White, A. H. *Aust. J. Chem.* **1998**, *51*, 433.

structure was solved by direct methods and refined by using a full-matrix anisotropic approximation for non-hydrogen atoms. All hydrogen atoms were placed in the structure factor calculations at idealized positions and were allowed to ride on the neighboring atoms with relative isotropic displacement coefficients.

**Acknowledgment.** This project was supported by the National Research Initiative of the USDA Cooperative State Research, Education and Extension Service, Grant No. 2003-35504-12846.

**Supporting Information Available:** Table giving $k_{obs}$ rate constants for reactions in eq 1 and a CIF file containing X-ray crystallographic data for complex **10**. This material is available free of charge via the Internet at http://pubs.acs.org.

OM061096U